Biogeosciences

Fluvial organic carbon fluxes from oil palm plantations on tropical peatland

Sarah Cook[1,2], Mick J. Whelan[2], Chris D. Evans[3], Vincent Gauci[4], Mike Peacock[5], Mark H. Garnett[6], Lip Khoon Kho[7], Yit Arn Teh[8], and Susan E. Page[2]

[1]Department of Engineering, University of Warwick, Coventry, CV4 7AL, UK
[2]Centre for Landscape & Climate Research, School of Geography, Geology and the Environment,
University of Leicester, LE1 7RH, UK
[3]Environment Centre Wales, Centre for Ecology and Hydrology, Bangor, LL57 2UW, UK
[4]Faculty of STEM, School of Environment Earth and Ecosystems, The Open University, Milton Keynes, MK7 6AA, UK
[5]Department of Aquatic Sciences and Assessment, Swedish University of Agricultural Sciences, 750 07, Uppsala, Sweden
[6]Natural Environment Research Council Radiocarbon Facility, Rankine Avenue, Scottish Enterprise
Technology Park, East Kilbride, G75 0QF, UK
[7]Tropical Peat Research Institute, Biological Research Division, Malaysian Palm Oil Board,
Bandar Baru Bangi 43000, Kajang, Selangor, Malaysia
[8]Institute of Biological and Environmental Sciences, University of Aberdeen, Aberdeen AB24 3UU, UK

Correspondence: Sarah Cook (sc606@le.ac.uk)

Abstract. Intact tropical peatlands are dense long-term stores of carbon. However, the future security of these ecosystems is at risk from land conversion and extensive peatland drainage. This can enhance peat oxidation and convert long-term carbon sinks into significant carbon sources. In Southeast Asia, the largest land use on peatland is for oil palm plantation agriculture. Here, we present the first annual estimate of exported fluvial organic carbon in the drainage waters of four peatland oil palm plantation areas in Sarawak, Malaysia. Total organic carbon (TOC) fluxes from the plantation second- and third-order drains were dominated (91 %) by dissolved organic carbon (DOC) and ranged from $34.4 \pm 9.7 \, \mathrm{C\,m^{-2}\,yr^{-1}}$ to 57.7 %, $16.3 \, \mathrm{g\,C\,m^{-2}\,yr^{-1}}$ ($\pm 95\,\%$ confidence interval). These fluxes represent a single-year survey which was strongly influenced by an El Niño event and therefore lower discharge than usual was observed. The magnitude of the flux was found to be influenced by water table depth, with higher TOC fluxes observed from more deeply drained sites. Radiocarbon dating on the DOC component indicated the presence of old (pre-1950s) carbon in all samples collected, with DOC at the most deeply drained site having a mean age of 735 years. Overall, our estimates suggest fluvial TOC contributes $\sim 5\,\%$ of total carbon losses from oil palm plantations on peat. Maintenance of high and stable water tables in oil palm plantations appears to be key to minimising TOC losses. This reinforces the importance of considering all carbon loss pathways, rather than just CO_2 emissions from the peat surface, in studies of tropical peatland land conversion.

1 Introduction

Tropical peat carbon stocks are estimated to be $105 \, \mathrm{Gt\,C}$ (105×10^{15} g; Dargie et al., 2017), with over half ($57 \, \mathrm{Gt\,C}$) stored within the peatlands of Southeast Asia (Page et al., 2011a; Dargie et al., 2017). Thus, Southeast Asian peatlands and tropical peatlands as a whole contain approximately 10 % and 20 % of the global peat carbon stocks, respectively (Page et al., 2011a; Dargie et al., 2017). Disturbance, including burning, deforestation, and drainage, often associated with land-use change, is common across the peatlands of Southeast Asia, driven by strong social and economic pressures to expand agricultural, palm oil, and pulpwood produc-

tion to support growing populations and economic development (Miettinen et al., 2012a). Consequently, only 6 % of remaining peat swamp forest areas are considered pristine (Miettinen et al., 2016), whilst carbon emissions from peatlands converted to agriculture are globally significant and increasing (Wijedasa et al., 2017).

Oil palm has played a central role in land-use change within Indonesia and Malaysia over the last few decades, driven by global consumer demand for vegetable-oil-based products and the exceptionally high productivity of oil palm compared to other oil-producing crops (Wicke et al., 2008, 2011; Schrier-Uijl et al., 2013; Gandaseca et al., 2014; Cole et al., 2015; Wijedasa et al., 2017). Over the next 30 years around 50 % of the remaining peat swamp forest in Indonesia is at risk of land conversion, predominantly for oil palm cultivation, despite a recent moratorium on the issuing of new concession licences for agriculture or logging in peatlands (Wijedasa et al., 2018). Peatland oil palm expansion is also prevalent within the Malaysian state of Sarawak (SarVision, 2011; Cole et al., 2015). By early 2016, nearly half (46 %) of the total peatland area in Sarawak was under industrial plantations, with 96 % of this area used for the cultivation of oil palm (Wetlands International, 2016).

The conversion of peat swamp forest to oil palm plantation involves a sequence of major disturbances, principally in the form of deforestation and drainage to optimise soil moisture conditions for cultivation (Hooijer et al., 2010; Page et al., 2011b; Schrier-Uijl et al., 2013). Prior to planting, peat surfaces are typically compacted using caterpillar-tracked vehicles in order to improve the rooting stability of the palms and to help with subsequent machinery movement during harvesting (Melling and Henson, 2011). These processes alter the peat's natural hydrological and biogeochemical functions, resulting in increased peat decomposition, loss of water storage and long-term subsidence (Hooijer et al., 2010; Tonks et al., 2017). This can give rise to oxidation of soil organic matter accumulated over millennia and to significant greenhouse gas (GHG) emissions (Couwenberg et al., 2010; Hirano et al., 2012). The result is often a reversal of the peatland carbon balance: from a net sink for atmospheric carbon to a net source (Miettinen et al., 2017). Managed land-use types now contribute to approximately 78 % of Southeast Asia's total GHG emissions related to peat oxidation (146 Mt C yr^{-1}; Miettinen et al., 2017).

Previous research on the effects of peat swamp forest disturbance has predominately focused on direct atmospheric GHG emissions from the peat surface (Couwenberg et al., 2010; Hooijer et al., 2010; Page et al., 2011; Hirano et al., 2012; Matysek et al., 2017). Until fairly recently, fluvial carbon losses received less attention, but more recent data suggest that this flux can represent a substantial fraction of the tropical peatland carbon balance (Moore et al., 2013; Evans et al., 2014; Rixen et al., 2016; Yupi et al., 2017). Fluvial total organic carbon (TOC) is typically dominated by dissolved organic carbon (DOC), with particulate organic carbon (POC) contributing < 10 % of the total flux (Moore et al., 2013; Yupi et al., 2017). Dissolved organic matter (DOM) is composed of a complex mixture of aromatic and aliphatic organic compounds, which have varying susceptibility to a range of physico-chemical and biological processes including photochemical degradation, flocculation, and microbial respiration, (Cory et al., 2014; Koehler et al., 2014; Catalán et al., 2015; Logue et al., 2016; Evans et al., 2017). Over 50 % of the organic carbon that is leached from tropical peat is believed to be subsequently mineralised and emitted to the atmosphere as CO_2 (Wit et al., 2015). These losses represent an important potential indirect contributor to GHG emissions. The riverine transport of TOC from land to ocean also represents a significant term in the global C budget (Ciais et al., 2013) and can have substantial impacts on the biogeochemistry and ecology of coastal waters (e.g. Frigstad et al., 2013).

Previous attempts to quantify fluvial carbon losses from tropical peatlands include Moore et al. (2013), Gandois et al. (2013), Wit et al. (2015), Rixen et al. (2016), and Yupi et al. (2016). Moore et al. (2013) reported that losses of DOC from disturbed tropical peatlands in Indonesia were around 50 % greater than those from an adjacent intact peat swamp forest. However, this research was based on a limited number of field sites (three intact sites and five degraded sites, all of which had unregulated drainage). Additional data are needed to better understand the dynamics of DOC in more intensively managed peatland environments with controlled drainage systems. This includes tropical peatland oil palm plantations where fluvial carbon losses remain unquantified. In addition, existing data demonstrate that the radiocarbon content of exported DOC (DO^{14}C) from intact tropical peat swamp forests is consistently modern (Moore et al., 2013; Gandois et al., 2013; Müller et al., 2015). DO^{14}C data for degraded tropical peatlands are more limited, particularly for peatland oil palm plantations. Moore et al. (2013) reported DO^{14}C data from five channels in drained and deforested peatlands in Indonesia, with mean ages of 92 to 2260 years BP, and two measurements from oil palm plantations in Peninsular Malaysia which had mean ages of around 3200 and 4200 years BP. These limited data clearly suggest that tropical peatland drainage releases DOC from long-term carbon stores but are insufficient to determine whether different forms of post drainage land use (e.g. oil palm cultivation versus abandonment) or hydrological management (e.g. regulated versus unregulated drainage) lead to different rates or age of DOC export. There is a particular need to acquire additional data from oil palm plantations as the most extensive, but currently under-represented, post-clearance land use on tropical peat.

In this paper, we quantify fluvial TOC concentrations, drainage channel discharge and fluvial TOC losses from four peatland oil palm plantations in Sarawak, Malaysia, over the course of 1 year. The main objectives of the study were (i) to quantify DOC and POC transfers in channels draining peat-
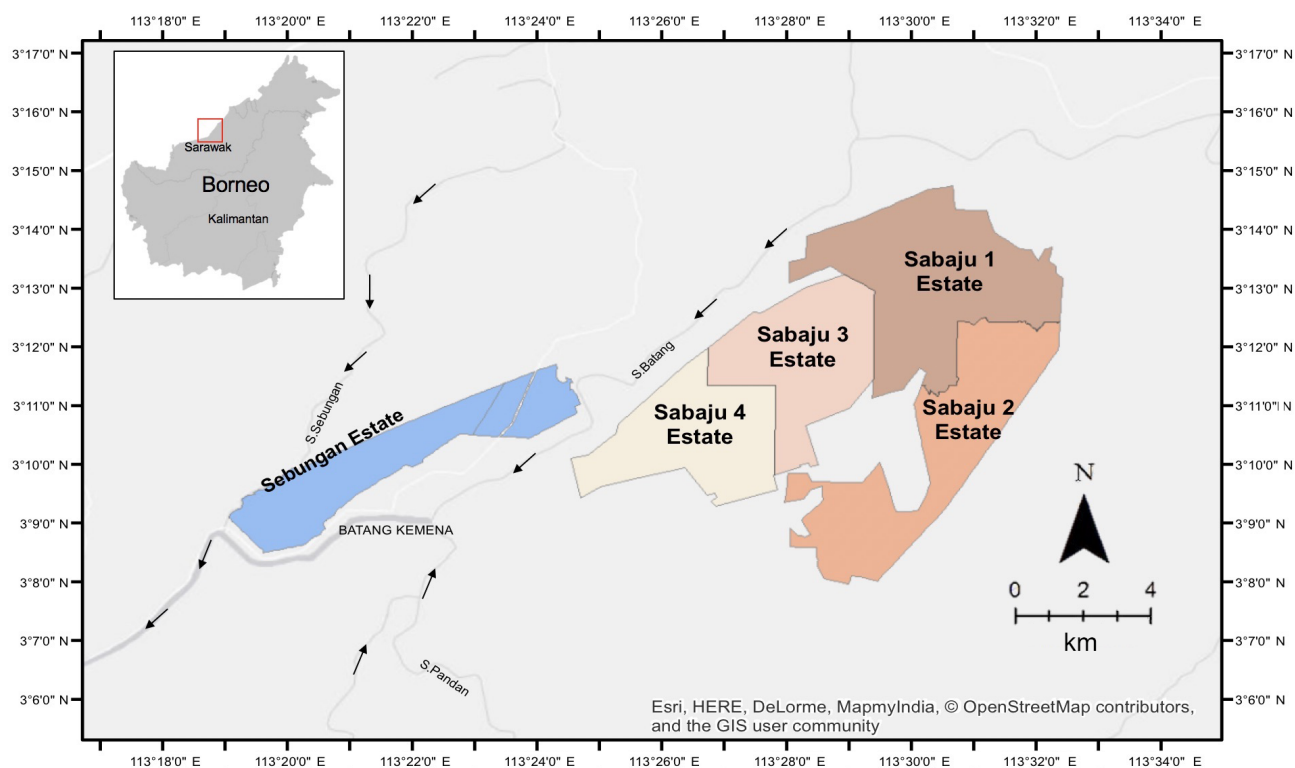
Figure 1. Location of the Sebungan and Sabaju oil palm estates, in Sebauh Bintulu district Sarawak, Borneo. The estates are bordered by a network of rivers (grey and white lines), namely the Batang Kemena, Sungai Sebungan, S. Batang, and S. Pandan. Arrows indicate direction of water flow.

land oil palm plantations, (ii) to derive annual area-specific TOC flux estimates from oil palm plantations for both the wet and dry seasons, and (iii) to establish the age and quality of the DOC being lost.

2 Materials and methods

2.1 Study site

The study was conducted in two adjacent oil palm estates: Sebungan (SE) and Sabaju (SA), situated in the Malaysian state of Sarawak, northern Borneo, east of the town of Bintulu (between $3°07.81'$ and $3°14.91'$ N and $113°18.72'$ and $113°32.19'$ E). The climate in this region is characterised by high temperatures (around $26\,°C$) throughout the year. Annual precipitation is typically between 3000 and 3200 mm (Environmental Impact Assessment, 2006). The annual rainfall pattern is influenced by the northeastern (October–January) and the southwestern (May–August) monsoons. The former is responsible for just under half of the annual rainfall, making this period the wettest, while the latter contributes around a quarter.

The estates cover a total area of 9614 ha. The Sebungan estate is established on an elliptical peat dome (Fig. 1) formed between two rivers (Batang Kemena and Sungai Sebungan),

which provide the main regional drainage for the plantation. The maximum peat depth is 5.6 m (Environmental Impact Assessment, 2006). Oil palm planting began in 2007 (making it the oldest plantation in this study) and the total planted area is 1648 ha. Due to the age of the plantation, the semi-mature palms provide a partially closed canopy (70 % closed) and some shade for the peat surface.

The Sabaju estate is divided into four individual oil palm plantations (Sabaju 1–4; Fig. 1). These are located on an irregularly shaped peat dome, with some small mineral soil hills protruding above the peat surface. Peat coring throughout the Sabaju estate has revealed very deep peat ($> 8\,\text{m}$) within Sabaju 4, moderately deep peat in Sabaju 3 ($\sim 4\,\text{m}$), and shallower peat in Sabaju 1 ($\sim 2\,\text{m}$). Sabaju 2 was excluded from this study due to the dominance of mineral soil. Of the three oil palm plantations under investigation (Sabaju 1, 3, and 4), the youngest palms were in Sabaju 4 (1638 ha), which was planted in 2011, followed by Sabaju 3 (1714 ha) planted in 2010. The oldest palms are located in Sabaju 1 (2526 ha) planted in 2008.

Plantation management on both estates is typical of other peatland oil palm plantations in this region. Artificial drainage networks have been established to lower water tables (with a target range of -60 to $-40\,\text{cm}$ below the peat surface to optimise palm growth). The drainage net-

works consist of a grid of interconnecting ditches (Fig. 2a). The edges of the planting blocks (approximately 19–50 ha in area) are defined by a set of roads that provide access (Fig. 2a). Each planting block contains multiple parallel "first-order" field drains (ditches approximately 0.5 m deep and 1 m wide) at a spacing of every four planting rows which feed into a central "second-order" collection drain (Fig. 2b). Second-order drains subsequently feed into a system of main "third-order" drains, which run parallel to the edge of the planting blocks. Water from the third-order drains feeds into perimeter (ring) drains, which discharge into the adjacent river network (Fig. 2b). The hydrology of these agricultural landscapes is intensively managed throughout the year. Channel gradients are low, which means that water depths and flow directions can be controlled via channel alterations (e.g. using sandbags and boards to narrow channels and or obstruct water flow) and the installation of weirs. This allows some mitigation for the effects of extreme environmental conditions, e.g. drought and flooding.

2.2 Water sample collection

A mixture of third-order (main) and second-order (collection) drains was monitored over an approximately 1-year (54-week) period, from 3 August 2015 to 8 August 2016, in the four main plantation study areas: Sebungan, Sabaju 1, Sabaju 3, and Sabaju 4. Sampling frequency was typically every 1–3 weeks. At each sampling, two water samples ($1 \times$ DOC; $1 \times$ POC) were collected from each of the monitored channels. Samples for DOC determination were collected in pre-rinsed 60 mL Nalgene® wide-neck bottles. Water samples for POC determination were collected using 500 mL plastic bottles. Water temperature (°C), pH, and electrical conductivity (EC; μS cm^{-1}) were recorded in the unfiltered water samples in situ, using a portable pH and EC probe (Hanna HI 9813-6).

DOC samples were filtered in a field laboratory through 0.45 μm cellulose nitrate membrane filters, which were pre-rinsed with sample, using a handheld vacuum pump, within 24 h of collection. After filtration, water samples were stored in the dark at 4 °C (for approximately 12 weeks), to ensure DOC preservation (Cook et al., 2016), before being shipped back to the UK. On return to the UK samples were analysed on a Shimadzu TOC analyser as non-purgeable organic carbon (NPOC) to generate measured DOC concentrations. See Supplement (Sect. S1) for further details.

POC concentrations were determined gravimetrically. Briefly, samples were filtered through 0.4 μm Advantec glass fibre filters which were dried for 3 h at 105 °C, weighed, and combusted in a furnace for a further 3 h at 550 °C and reweighed. The particulate organic matter (POM) concentration was calculated from the difference in the filter mass between oven-drying and combustion divided by the volume filtered. This was subsequently converted into POC assum-

ing a 50 % organic carbon content (Hope et al., 1994; Moore et al., 2011).

2.3 Carbon quality

The nature of the DOC sampled was investigated using SUVA$_{254}$ (specific ultraviolet absorption). This is the ultraviolet (UV) absorbance at 254 nm normalised to sample DOC concentration (Weishaar et al., 2003). Absorbance at 254 nm is commonly used as a surrogate for DOC aromaticity, i.e. the fraction of DOC comprised of aromatic humic substances, which absorb light in this particular part of the electromagnetic spectrum. High-SUVA$_{254}$ compounds tend to be more photodegradable and low-SUVA$_{254}$ compounds more biodegradable (Jones et al., 2016).

UV–vis absorbance was measured using a Cole-Parmer UV–visible spectrophotometer (230 VAC, 50 Hz) at 254 nm. Samples were analysed immediately after filtration. SUVA$_{254}$ values (l mg C^{-1} m^{-1}) were calculated from

$$\text{SUVA}_{254} = 100 \times \frac{A_{254}}{C_{\text{DOC}}}, \tag{1}$$

where A_{254} is absorbance at 254 nm and C_{DOC} is the DOC concentration (mg C l^{-1}), after Weishaar et al. (2003). Water samples with very high absorbance at 254 nm (> 3.0) saturated the spectrophotometer and were therefore removed from the data set ($n = 1$) prior to analysis.

2.4 Hydrology

Drainage channel discharge was determined periodically at a number of locations under different conditions using dilution gauging (Hongve, 1987; Hudson and Fraser, 2002). Briefly, a sodium chloride tracer solution was injected into the flow and the consequent concentration change was observed at a point downstream (~ 30 m; assuming full mixing has occurred). EC was used as a surrogate for concentration via site-specific concentration–conductivity calibrations. This technique is considered by us to be superior to methods based on cross-sectional area and velocity measurements in shallow, irregular channels. The measured discharge data were used to construct rating curves (stage–discharge relationships) for each location, for which stage height was measured from stage boards, which were calibrated against semi-continuous recordings of water level measured at 1 h intervals using atmosphere-corrected pressure transducers (Mini-Divers, Schlumberger, D1501) installed in stilling wells. Whenever water samples were collected, the stage was noted and converted to discharge using the rating curve. The rating curve equations for all measured sites, along with the standard error of the estimate (SEE) derived from the regression equations, are presented in the Supplement (Table S1; Figs. S1 to S3). The stage records from the Mini-Divers were used to reconstruct a continuous record of discharge for eight stations throughout the year from 15 September 2015 until 31 August 2016.
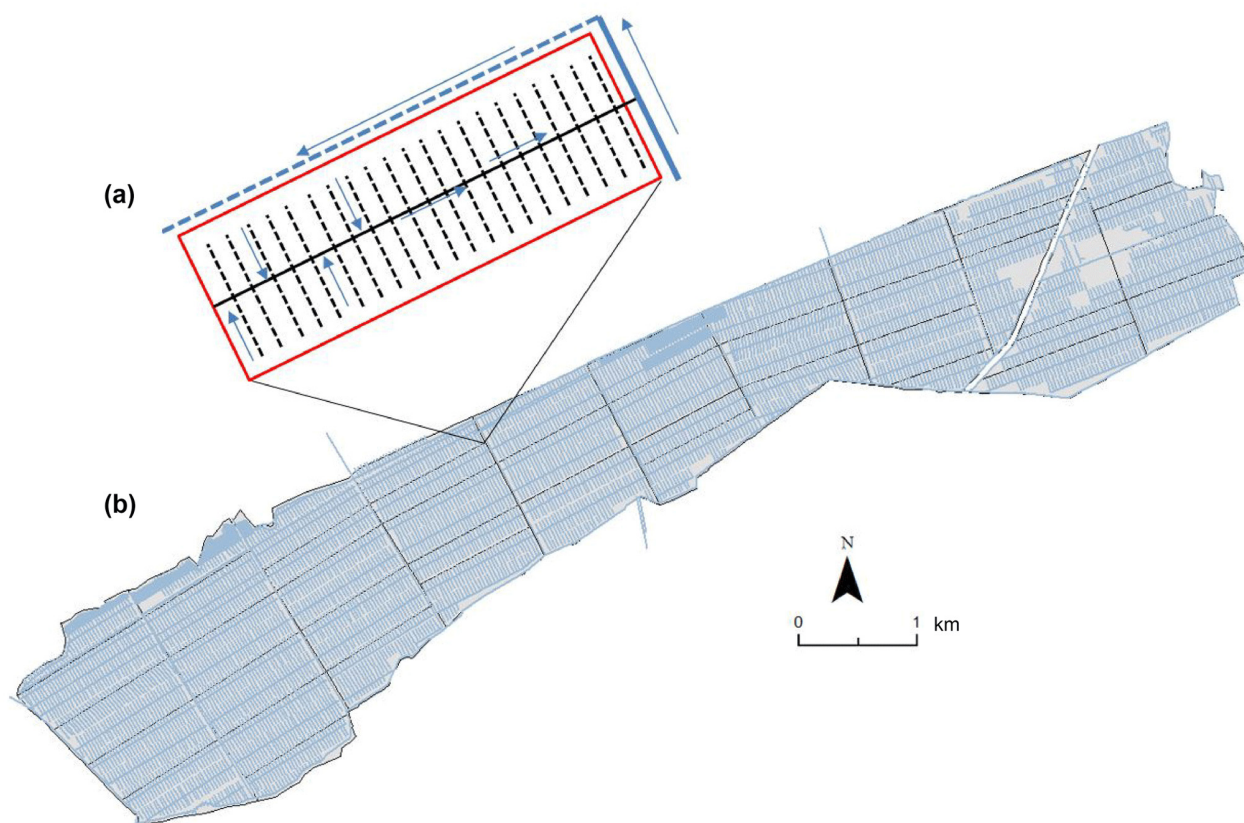
Figure 2. Example of **(a)** peatland oil palm plantation (Sebungan estate) layout with the planting blocks, drains, and roads highlighted and **(b)** close-up schematic of a typical drainage set-up on a peat oil palm planting block. Red box: planting area; black dashed line: first-order field drains; solid black line: second-order collection drain; solid blue line: third-order main drain; blue dashed line: perimeter drain. Arrows show the prevailing direction of water flow

Peatland water table depths (below the peat surface) were determined using dip wells constructed from 32 mm diameter PVC tubes cut to 2 m lengths. Spaced at 35 mm intervals, 5 mm holes were drilled down each tube. The top of each tube was fitted with a removable cap to allow access to the tube but prevent rain and debris from entering between measurements. The bottom of each tube was fitted with a glued PVC plug to prevent sediment encroachment. A cluster of three dip wells (inserted 1.5 m into the peat from the surface, at 0.5 m intervals from one another) was installed in the centre of one planting block at each plantation study site. Measurements of water table depths were made using a dipmeter (in situ rugged water level tapes) in each field sampling visit, at the same time as water samples were collected.

2.5 Flux calculation

The annual area-specific TOC flux (J: $\mathrm{g\,C\,m^{-2}\,yr^{-1}}$) for each station was calculated from

$$J = C_W \times R_E = \frac{\sum(C_i \times Q_i)}{\sum Q_i} \times R_E, \qquad (2)$$

where C_W ($\mathrm{g\,C\,m^{-3}}$) is the annual flow-weighted concentration, C_i ($\mathrm{g\,C\,m^{-3}}$) is the instantaneous (sampled) concentration of TOC (DOC + POC) on sampling date i, Q_i is the corresponding discharge at time of sampling ($\mathrm{m^3\,s^{-1}}$), and R_E is the annual run-off ($\mathrm{m\,yr^{-1}}$). R_E can be calculated from measured channel discharge and catchment area:

$$R_E = \frac{\sum Q_A}{A} = \frac{\sum\limits_{h}^{T} Q_h}{A}, \qquad (3)$$

where Q_A is the measured mean annual discharge ($\mathrm{m^3\,yr^{-1}}$) estimated as the sum of hourly discharge h (Q_h; $\mathrm{m^3\,h^{-1}}$) over T hours in the measurement period, and A is the catchment area ($\mathrm{m^2}$).

In principle, the catchment area for a particular drain can be estimated from the topography of the plantation block areas which it serves. However, because channel gradients in peatland landscapes are low, this is subject to a high level of uncertainty, particularly for lower-order drains. Consequently, we applied a water balance approach to the calculation of discharge. To do this, R_E was assumed to be the same

for all plantation sites, based on the assumption that all sites were hydrologically similar in terms of the annual water balance. While this is a simplistic approach all sites had similar soil properties, topography, vegetation, and management and were sufficiently close together such that they experienced very similar rainfall. By also assuming no annual change in catchment water storage (the average difference between water table depth at the beginning and end of the monitoring period was ~ 30 mm, implying that any storage changes were on the order of 10 s of mm), R_E can be calculated from climate data using

$$R_E = P - ET_a, \tag{4}$$

where P is the annual rainfall (mm yr^{-1}) and ET_a is the annual actual evapotranspiration (mm yr^{-1}), which was calculated from

$$ET_a = k_C\ ET_0, \tag{5}$$

where k_C is the so-called "crop coefficient" and ET_0 is the annual reference evapotranspiration rate (a standardised ET rate which assumes soil moisture is not limiting).

ET_0 (mm yr^{-1}) was calculated from average daily values of temperature, relative humidity, wind speed, and net radiation flux density using the Penman–Monteith equation (e.g. Monteith, 1965). Meteorological data (including P) were available over the period from 15 September 2015 to 6 August 2016 from an on-site automatic weather station (Davis Vantage Pro 2). Carr (2011) reports that k_C for oil palms typically varies between 0.8 and 1 when soil moisture is unlimited in the wet season. Lower k_C values have been reported in the dry season for other areas. However, although the near-surface peat layer does dry out seasonally, palm oil roots generally extend much deeper (i.e. 50–70 cm; Othman et al., 2010; Veloo et al., 2015) – into or close to the saturated zone. We therefore assumed that soil moisture availability is rarely limiting and adopted a value of 0.9 for k_C over the whole year. This assumption was supported by water balance modelling following the method of Whelan and Gandolfi (2002), which showed that measured discharge at all Sebungan monitoring stations could be simulated well with $ET_a - 0.9\,ET_0$ over the whole year (data not shown).

2.6 Flux uncertainty

TOC fluxes were subject to considerable uncertainties, specifically in (i) DOC concentration, (ii) the mean annual run-off (R_E) and (iii) channel discharge at the time of sampling (Q_i). These were accounted for in our overall flux estimates using a Monte Carlo simulation approach as detailed below.

2.6.1 Monte Carlo simulation

The second-order drain with the most reliable catchment area was SE 1 (2 167 300 m^2). This was defined topographically

during a field reconnaissance in April 2015 in which water flow directions and the drainage layout were mapped manually and then digitised in ArcGIS. A value of R_E was then calculated by applying Eq. (3) for the period for which complete meteorological data were available (15 September 2015 to 6 August 2016) and for the whole year (discharge measurements were available for the whole year). Their associated error was then estimated using standard errors derived using a Monte Carlo error propagation simulation (e.g. Iman and Conover, 1980; Farrar et al., 1989) in which the error in Q_h (± 15.14 m^3 h^{-1}) was assumed to be the standard error of the estimate in the rating curve for SE 1 and in which an error of 25 % was arbitrarily (and conservatively) assumed for A. Briefly, values for each variable were selected randomly from probability density functions (PDFs) and employed in Eq. (3) in a large number (5000) of iterations. Gaussian PDFs were used based on the assumption that the estimate of a statistic is normally distributed about the true value (central limit theorem) with the best-estimate value assumed for the mean and SEE assumed for the standard deviation. This is described in more detail in the Supplement (Sect. S2; Figs. S4–S7).

The following variables were sampled from their PDFs in calculating flux uncertainty in Eq. (2) for each plantation area: C_i, Q_i, and R_E. Variances for Q_i and C_i were derived, respectively, from (i) the SEE values given in the regression equations for the rating curves and (ii) the error associated with the DOC concentrations obtained using the TOC analyser (assumed to be the true value) with a precision of ~ 5 % (Graneli et al., 1996; Bjorkvald et al., 2008; Shafer et al., 2010). This is detailed in the Supplement (Sect. S1).

2.7 Radiocarbon dating (DO^{14}C)

Water samples for radiocarbon dating were acquired from three second-order drains within both the Sebungan and Sabaju 3 plantations (six samples in total). Sample collection from third-order (main) drains was avoided to prevent pseudo-replication (i.e. nested catchments). All samples were collected over the course of 24 h in the wet season (April 2016) in pre-rinsed (with sample) 500 mL polypropylene bottles and filtered using a 0.7 µm glass fibre filter. These filters were pre-combusted at high temperatures (450 °C) to minimise the organic matter contamination risk. The water samples were stored at 4 °C for approximately 1 year prior to analysis. Cold storage has been shown to be a viable method for the long-term preservation of carbon isotopic signatures (Gulliver et al., 2010). Samples were analysed by accelerator mass spectrometry (AMS) at the Natural Environment Research Council facility in East Kilbride, UK, in 2017. Values were expressed as % modern (m) or conventional radiocarbon ages (in years BP, where 0 BP = 1950 CE = 100 % modern):

$$\text{age(years BP)} = -8033 \times \ln(m/100) \tag{6}$$

$$m = \left(\frac{A_{\text{SAMPLE}}}{A_{\text{OXALIC}}}\right) \times 100,$$

where A_{SAMPLE} is the ^{14}C-normalised radioactivity in the sample and A_{OXALIC} is the ^{14}C-normalised radioactivity in the oxalic acid international radiocarbon standard with a radioactivity equivalent to the atmosphere in 1950 (i.e. 100 % modern = year 1950 CE).

2.8 Age attribution model

DOC in water samples contains a mixture of organic matter from old (^{14}C depleted) peat and recently photosynthesised (^{14}C enriched) litter and plant material (Evans et al., 2014; Campeau et al., 2017). Ascribing a "mean age" to carbon fixed post-1950 is complicated by nuclear bomb testing, which released a pulse of enriched ^{14}C into the atmosphere. The ^{14}C isotopic signature is, therefore, likely to reflect a mixture of both old (pre-1950's) and new (post-bomb/^{14}C-enriched) carbon, in varying amounts. Thus, no single definitive mean age can be ascribed to the sample (Evans et al., 2007). To address this, the age attribution model previously described by Moore et al. (2013) and Evans et al. (2014) was used to infer an indicative age distribution for the DOC in the samples. The model assumes an exponential decrease in the amount of DOC produced with increasing depth (and therefore age) within the peat profile. Each year class in the profile was assigned a ^{14}C value based on estimated atmospheric CO_2 for that year (see Evans et al., 2014) and the maximum age was set to 4300 years BP, based on ^{14}C basal ages recorded for this region by Dommain et al. (2011). The model can be expressed as

$$\text{DO}^{14}\text{C} = \sum_{t=1}^{t=4300} \left(14\,\text{CO}_2 t \times e(-k \times t)\right), \tag{7}$$

where DO^{14}C is the measured ^{14}C of the DOC sample, t is year prior to present day, $^{14}\text{CO}_{2t}$ is the ^{14}C level of atmospheric CO_2 in year t, and k is an exponential decay constant with a value between 0 and 1. For each sample, k was adjusted to fit measured DO^{14}C using an iterative optimisation routine (Microsoft Excel Goal Seek). Modelled age distributions were summarised by aggregating year classes into the age categories 0–9, 10–49, 50–99, 100–299, 300–499, 500–699, 700–999, 1000–2999, and > 3000 years.

2.9 Bulk density and aerated carbon stocks

Bulk density (BD) was determined on four peat cores (up to 4 m in length) per plantation, extracted using a Russian corer. Subsamples of 123 cm^3 in volume were taken every 15 cm down to the water table (identified using a dipmeter) and every 50 cm thereafter. A total of 47 peat samples were oven-dried at 105 °C for up to 120 h (until the dry weight
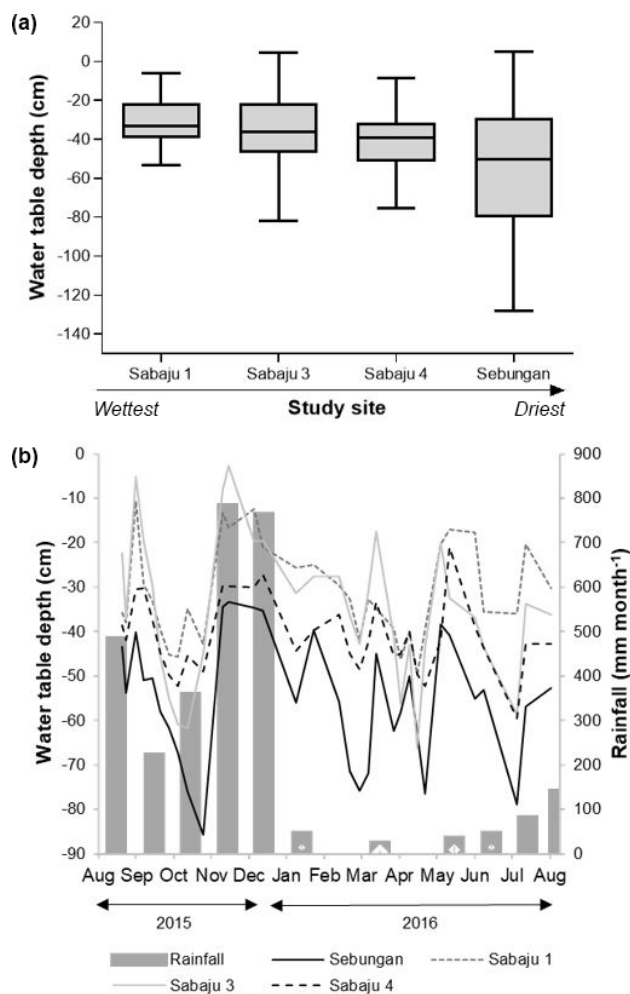

Figure 3. Water table depths measured in dip wells in all monitored areas, presented as **(a)** box plots showing mean water table depths for all monitored plantations over the study period (August 2015–September 2016) (central horizontal line), along with the minimum and maximum depths recorded over the entire study period (bars). The box shows the 75th and 25th percentiles, positioned in sequence from the highest to lowest water table, and **(b)** as a time series of mean weekly water table depths. Negative values indicate that the water table was below the peat surface; positive values indicate that there was standing water above the peat surface. Monthly rainfall data were obtained from the rainfall gauge at the Sebungan plantation base (August 2015–August 2016).

of the sample had stabilised) and weighed to calculate the BD. The total aerated carbon stock SOC_{air} (kg m^{-2}) for each plantation was then derived (Tiemeyer et al., 2016) as

$$\text{SOC}_{\text{air}} = \frac{z_{\text{WT}}}{n} \sum \rho_j\,\text{SOC}_j, \tag{8}$$

where ρ_j (g cm^3) is bulk density for sample j, SOC_j is the soil organic carbon content (g kg^{-1}) of sample j (derived from loss on ignition assuming 50 % carbon), n is the num-

ber of samples collected above the water table and z_{WT} is the average annual water table depth (m).

2.10 Statistical analysis

Statistical analysis was performed using GraphPad Prism v7. The threshold level of statistical significance was set at a probability of 0.05 but greater significance was also noted. For multiple comparisons, one-way ANOVAs were performed. The assumptions that the data adhered to normality and homogeneity of sample variance were checked a priori using the Shapiro–Wilk and Bartlett tests, respectively. If significant differences between the group means were identified then a post hoc test was carried out. In cases in which these assumptions were not valid, the non-parametric Kruskal–Wallis test was performed together with a post hoc test as above. In addition, the relationship between variables was tested using linear regression models.

3 Results

3.1 Water table depths and aerated carbon stocks

Mean water table depths for the individual estates are displayed in Fig. 3 and Table 1. The lowest mean water table (i.e. furthest from the peat surface) was observed in the Sebungan estate (-55 cm; Fig. 3a). The highest mean water table (i.e. closest to the peat surface) was observed in Sabaju 1 (-31 cm; Fig. 3a). The SE site displayed the greatest degree of water table variability, with depths ranging from -128 cm to $+5$ cm (i.e. above the peat surface). This was closely followed by Sabaju 3, where water depths ranged from -82 to $+4$ cm. The lowest variability was observed at Sabaju 1 where the water table depth varied between -53 and -6 cm. Seasonal variations in water table followed monthly rainfall (Fig. 3b). A relationship between the rainfall pattern and temporal variability in the water table depth could not be drawn due to differences in the data resolution (i.e. water tables were only sampled weekly, which did not necessarily capture the full variability in the rainfall).

BD measurements revealed higher compaction of the near-surface peat within the Sebungan estate compared to that in the Sabaju estate; the average BD for the upper 1 m of peat in the Sebungan estate was 0.18 ± 0.01 g cm^{-3} (standard error), compared to an average BD value for the Sabaju estate of 0.10 ± 0.01 g cm^{-3} (Table 1). Overall, BD ranged from 0.06 ± 0.01 to 0.24 ± 0.01 g cm^{-3} across all samples. Similarly, the Sebungan estate displayed a higher overall SOC$_{air}$ value of 45.3 kg m^{-2}, which was more than double the SOC$_{air}$ values calculated for the three Sabaju estates (14.2 to 18.9 kg m^{-2}; Table 1).
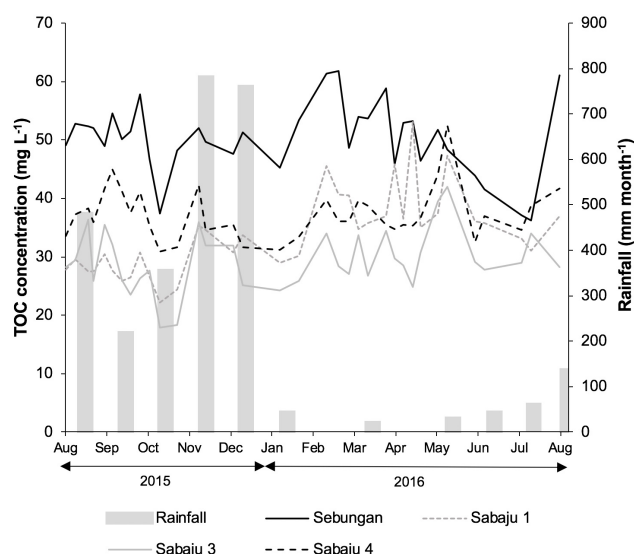

Figure 4. Weekly TOC concentration data for the study plantations, alongside monthly rainfall. Data presented are mean weekly TOC concentrations from all drains within each site. Monthly rainfall data were obtained from the rain gauge at the Sebungan plantation base (August 2015–August 2016).

3.2 Catchment hydrology

Mean calculated totals for P, ET$_0$, ET$_a$, and R_E over the period 15 September 2015 to 6 August 2016 were 2046, 1135, 1021, and 1025 mm, respectively. The value for P was much lower than the typical annual value in the region (ca. 3000 mm yr^{-1}). This was due to the influence of the 2015–2016 El Niño event characterised by extended dry periods. The calculated R_E was 1022 ± 55 mm for the period for which complete meteorological data were available and 1090 ± 147 mm yr^{-1} for the whole year. These values match the R_E estimate derived from the water balance (1025 mm), lending confidence to our estimates of TOC fluxes.

3.3 Fluvial organic carbon

Mean annual TOC concentrations ranged from 29.3 to 51.2 and 29.6 to 49.6 mg l^{-1} in the second-order collection drains and third-order main drains, respectively (Table 2). The Sebungan plantation sites displayed the highest TOC concentrations and those in Sabaju 3 the lowest (Table 2). Concentrations in both the main and collection drains at Sebungan were significantly different to all the other plantation sites ($p < 0.0001$, unpaired Kruskal–Wallis). DOC was always the dominant component of TOC, accounting for 84 %–95 % of TOC (Table 2). Overall, there were no significant seasonal temporal trends in TOC concentrations, which remained relatively stable for the duration of the investigation (~ 30 to 50 mg l^{-1}; Figs. 4 and 5). This is seen in contrast to the discharge (Fig. 5). There were no systematic differences in

Table 1. Mean water table, bulk density, and SOC_{air} measurements for the four oil palm plantations; $\pm$ represents the standard error of the mean.

Plantation	Mean water table depth (cm)	Average bulk density ($g\,cm^{-3}$)		SOC_{air} ($kg\,m^{-2}$)
		Whole core	Top 1 m of peat	
Sabaju 1	31.3 ± 1.1	0.095 ± 0.008	0.102 ± 0.009	14.7 ± 1.6
Sabaju 3	35.1 ± 1.8	0.081 ± 0.005	0.098 ± 0.007	14.2 ± 2.3
Sabaju 4	40.9 ± 1.7	0.092 ± 0.005	0.103 ± 0.012	18.9 ± 1.2
Sebungan	55.3 ± 3.3	0.165 ± 0.008	0.182 ± 0.007	45.3 ± 2.1
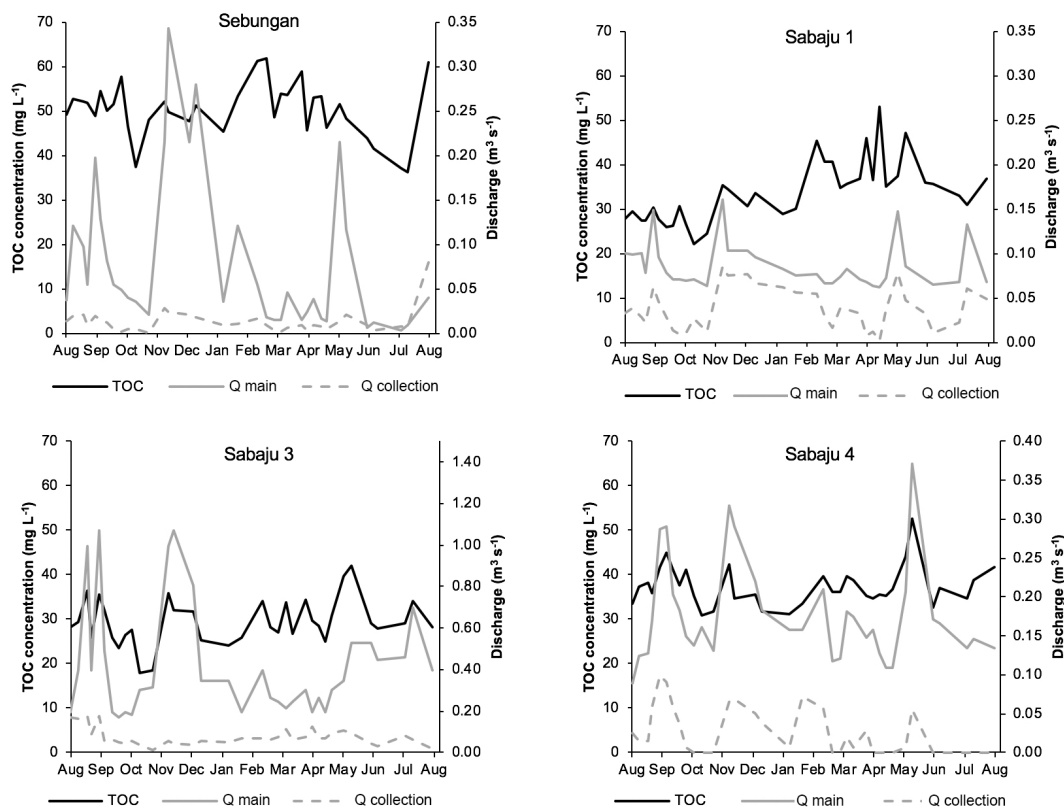
Figure 5. Weekly TOC concentration data for the study plantations, alongside the mean discharge (Q, $m^3\,s^{-1}$) for the monitored main and collection drains within each plantation estate (August 2015–August 2016).

$SUVA_{254}$ among the different estates or between second and third-order drains.

TOC fluxes were determined for all individual plantations except for three second-order drains (one in Sabaju 1 and two in Sabaju 3), which experienced significant changes in their hydrological regimes as a result of plantation management actions. These actions included channel blocking and widening, which led to complications in estimating discharge and therefore TOC fluxes. Mean annual TOC fluxes ranged from 34.4 ± 9.7 to $57.7 \pm 16.3\,g\,C\,m^{-2}\,yr^{-1}$ (Fig. 6; Table 2; see Table S2 for individual site fluxes,), with significantly higher fluxes ($p < 0.05$, unpaired, one-way ANOVA) recorded in the Sebungan plantation Sabaju 3 (Fig. 6). Mean annual TOC losses were 44.7 ± 12.6 and $42.1 \pm 11.9\,g\,C\,m^{-2}\,yr^{-1}$ from

the second- and third-order drains, respectively. The two components of TOC (DOC and POC) contributed 9 % and 7 %, respectively, on average to annual TOC yields across all plantation sites, with a slightly higher contribution from DOC to TOC in the second-order drains (91 % third order vs. 94 % second order).

3.4 $DOC^{14}C$

The greatest ^{14}C enrichment was exhibited by site SA 3.6 (102.6 % modern) and the greatest ^{14}C depletion by site SE 4 carbon (91.3 % modern; Table 3). Conventional mean $DO^{14}C$ age was positively correlated ($p < 0.05$) with the depth of the water table and drainage intensity (Table 3; Fig. 7), but this

Table 2. Fluvial organic carbon data for the monitored oil palm plantations. DOC, POC, and TOC concentrations and $SUVA_{254}$ are shown as site mean ± standard error of the mean. Annual TOC fluxes are shown as site mean ± the 95 % confidence interval (CI; standard error × 1.96), which encompasses the propagated error associated with uncertainty in the DOC concentration, discharge, and annual run-off derived from the Monte Carlo simulation. $SUVA_{254}$ values are means of samples collected for each drain type in each plantation throughout the sampling year.

Plantation	Drain type	No. of channels	Mean DOC concentration $(mg\,l^{-1})$	Mean POC concentration $(mg\,l^{-1})$	Mean TOC concentration $(mg\,l^{-1})$	Annual TOC flux $(g\,C\,m^{-2}\,yr^{-1})$	$SUVA_{254}$ $(L\,mg\,C^{-1}\,m^{-1})$
Sabaju 1	Collection (second order)	2	31.1 ± 1.1	2.7 ± 0.3	33.8 ± 1.1	38.2 ± 10.8	5.2 ± 0.1
	Main (third order)	1	29.7 ± 0.9	3.9 ± 0.5	33.6 ± 0.8	36.8 ± 10.5	5.2 ± 0.1
Sabaju 3	Collection (second order)	2	25.2 ± 0.8	4.1 ± 0.3	29.3 ± 0.7	36.4 ± 10.3	5.4 ± 0.1
	Main (third order)	1	25.0 ± 1.0	4.6 ± 0.5	29.6 ± 1.1	34.5 ± 9.7	5.1 ± 0.1
Sabaju 4	Collection (second order)	2	34.1 ± 0.6	2.5 ± 0.3	36.7 ± 0.6	42.1 ± 11.9	5.0 ± 0.1
	Main (third order)	2	35.3 ± 0.6	2.7 ± 0.3	38.0 ± 0.7	43.1 ± 12.2	5.6 ± 0.1
Sebungan	Collection (second order)	3	48.2 ± 0.8	3.4 ± 0.4	51.2 ± 1.0	56.3 ± 15.9	5.6 ± 0.2
	Main (third order)	1	47.1 ± 0.8	2.5 ± 0.2	49.6 ± 0.8	53.0 ± 15.0	6.4 ± 0.1

Table 3. Mean and standard errors for radiocarbon $DO^{14}C$ expressed as % modern and in conventional radiocarbon years (years BP, relative to CE 1950), expressed at the ± 1σ level, for individual sample sites across the Sebungan (SE 2, SE 3, SE 4) and Sabaju 3 (SA 3.1, SA 3.3, SA 3.6) estates. Mean ^{14}C levels > 100 % modern cannot be assigned an age and are subsequently referred to as "modern". Mean annual water table depth data for each site are also presented, along with the maximum and minimum water table depths recorded and the % of time the water table was more than 60 cm from the peat surface. Negative numbers indicate distance below the peat surface.

Plantation	Sample site	^{14}C (% modern)	$DO^{14}C$ Age (years BP)	Water table depth (cm) Mean	Maximum	Minimum	% of time water table was below −60 cm
Sebungan	SE 2	100.10 ± 0.46	modern	−21	5	−58	0 %
	SE 3	99.57 ± 0.46	35 ± 37	−52	−34	−89	27 %
	SE 4	91.26 ± 0.42	735 ± 37	−92	−65	−128	100 %
Sabaju 3	SA 3.1	102.37 ± 0.47	modern	−30	4	−56	0 %
	SA 3.3	99.63 ± 0.44	30 ± 35	−39	4	−82	21 %
	SA 3.6	102.63 ± 0.47	modern	−36	−14	−72	3 %

was strongly dependent on site SE 4, which had the deepest average drainage depth and greatest ^{14}C depletion, corresponding to a mean $DO^{14}C$ age of 735 ± 37 years BP (Table 3). The other five sites were all wetter (average water tables −21 to −50 cm) and clustered within a fairly narrow $DO^{14}C$ range (99.6–102.6 % modern).

The fitted age attribution model (Fig. 8) suggests that the majority of DOC in all samples, other than SE 4, originates from peat with a ^{14}C age of 100–500 years BP. Based on its lower measured ^{14}C value, the SE 4 sample is estimated to contain a larger proportion of older peat carbon, with > 35 %
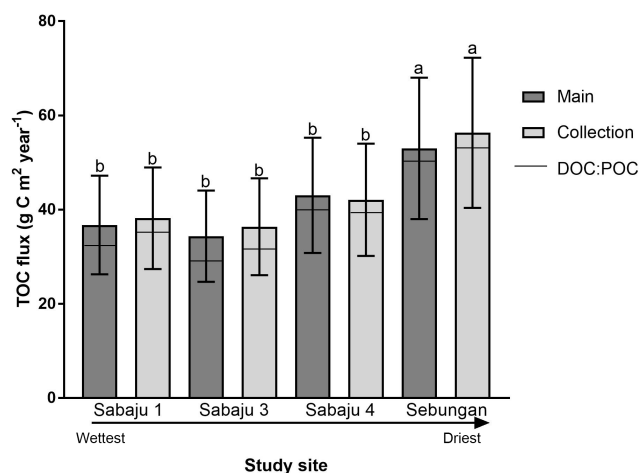
Figure 6. Mean annual TOC fluxes for the plantation drains. Error bars represent ± the 95 % confidence interval (CI; standard error × 1.96), which encompasses the propagated error associated with uncertainty in the DOC concentration, discharge, and annual run-off derived from the Monte Carlo simulation. Fluxes are separated into the different drain types: third order (main) and second order (collection). Horizontal bar lines represent contribution of DOC (bottom segment) and POC (top segment) to the overall TOC flux. Estates are presented in sequence of drainage intensity. Letters "a" and "b" denote significant differences ($p < 0.05$, unpaired, one-way ANOVA) across the study sites irrespective of drain type.
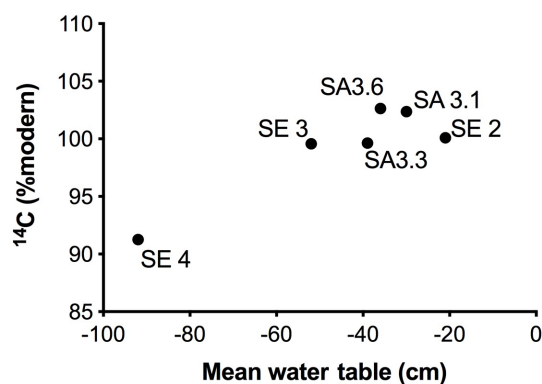
Figure 7. Mean water table depths plotted against ^{14}C (% modern) for all six sites in the Sebungan (SE 2, SE 3, SE 4) and Sabaju 3 (SA 3.1, SA 3.3, SA 3.6) estates. Negative numbers denote distance below the peat surface.

estimated to be derived from material with a ^{14}C age exceeding 1000 years BP.

4 Discussion

Average DOC concentrations in water draining the Sabaju oil palm plantations were lower than those reported by Moore et al. (2013) for drained tropical peatlands (ca. 52 mg l^{-1}), while those from the Sebungan plantation were in line with

the values reported by Moore et al. (2013). The average annual TOC fluxes (Fig. 6) for the third-order (main) and second-order (collection) drains were also less than TOC flux estimates for drained tropical peat swamp forests reported elsewhere (94 to 108 g C m^{-2} yr^{-1}; Moore et al., 2013; Müller et al., 2015) and those reported for intact peat swamp forests in Indonesia and Sarawak, Malaysia (63–64 g C m^{-2} yr^{-1}), by Moore et al. (2013) and Müller et al. (2015). The annual Sebungan estate TOC fluxes were significantly higher than the fluxes from the Sabaju estate (Fig. 6). The lower annual fluxes (for drained tropical peat) reported here reflect a combination of relatively low TOC concentrations (e.g. compared to Moore et al., 2013) and relatively low total annual run-off during the study period. The latter was influenced by an El Niño-driven drought event (i.e. low rainfall recorded in 2016; Fig. 3b). Since discharge varies much more than DOC concentration (Fig. 5), the temporal pattern of DOC fluxes from the study catchments is primarily controlled by discharge (Clark et al., 2007). Initial plantation development on tropical peat is often associated with the release of large pulses of carbon due to enhanced mineralisation during the first 5 years (Hooijer et al., 2010; Page et al., 2011b). Since the plantations which were sampled here were 6 to 9 years old, these initial responses to disturbance are unlikely to have been captured. Together with the low (El Niño-related) rainfall and run-off rates experienced, our flux estimates are, therefore, probably relatively conservative of fluvial TOC losses from oil palm plantations overall. Reported peat surface CO_2 emissions from oil palm plantations are typically in the range of 900 to (Husnain et al., 2014) to 2700 g C m^{-2} yr^{-1} (Hooijer et al., 2012). As such, the TOC fluxes reported from this study could represent an additional carbon loss equal to $\sim$ 2 % to 5 % of total carbon emissions from oil palm plantations on peat.

The spatial variations in the TOC flux across the four monitored oil palm plantations (Fig. 6) were principally controlled by DOC concentrations which, in turn, appeared to be related to water table depth, with higher DOC concentrations and fluxes from the deep-drained Sebungan site compared to the shallower-drained Sabaju sites (Figs. 3 and 5; Tables 2 and 3). This is broadly consistent with the conclusions of previous analyses of peatland drainage impacts on DOC loss (Evans et al., 2016), but contrasts somewhat with the assessment by Moore et al. (2013), which recorded higher DOC fluxes (principally due to higher water losses) but not higher DOC concentrations. Conversely, Yupi et al. (2017) did record higher DOC concentrations as well as fluxes from a small drainage-affected catchment, compared to a river draining a larger, relatively intact peat swamp forest. Differences between our results and those of Moore et al. (2013) may be explained by differences between the study areas; the Moore et al. (2013) study compared highly contrasting sites (drained and deforested versus undrained natural forest) with large resulting differences in water balance. In contrast, our study compared sites with differing drainage depths within
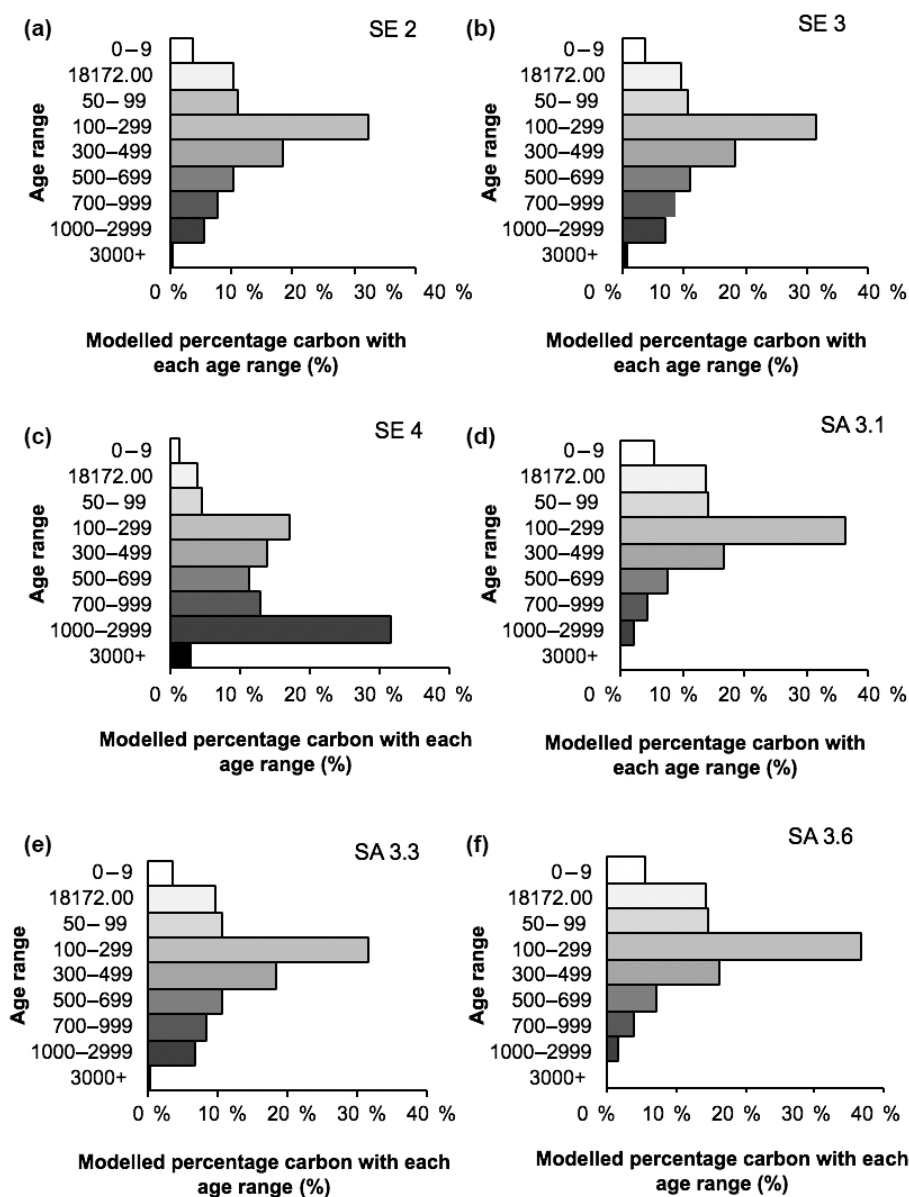
Figure 8. Modelled age distributions of DO^{14}C, as estimated from the age attribution model for all radiocarbon-dated water samples ($n = 6$) in the Sebungan (SE 2, SE 3, SE 4) and Sabaju 3 (SA 3.1, SA 3.3, SA 3.6) estates.

a single land-use category and consequently a more uniform water balance. Conversely, we observed variations in DO^{14}C versus drainage depth that were consistent with those observed elsewhere in both tropical and high-latitude peatlands (Evans et al., 2014) (Fig. 7 and Table 3). This clearly suggests that deeper drainage leads to the mobilisation of older peat C into DOC and is also associated with the release of more humified (high SUVA$_{254}$) material, consistent with previous findings (Olefeldt et al., 2013). In general, our observed SUVA$_{254}$ values were higher than those reported previously in run-off from intact peat swamp forests (Moore et al., 2013; Gandois et al., 2013), which can be explained by a transition

from plant-derived to peat-derived DOC sources following forest clearance and drainage (Könönen et al., 2016).

The differences in water table depth (Fig. 3) between the Sabaju and Sebungan estates are further accentuated by the differences in bulk density, potentially leading to large differences in SOC$_{air}$ (Table 1). This suggests a denser concentration of carbon in the peat above the water table (i.e. higher SOC$_{air}$), which could promote higher rates of organic matter decomposition and, hence, TOC production in the Sebungan estate. However, as peat carbon content was not measured the link between peat bulk density and the TOC fluxes cannot be fully established. The differences in these bulk densi-

ties could originate from differences in the site management, plantation age, or intrinsic differences in the peat characteristics between the two peat domes.

Overall, our results suggest that the clearance and drainage of peat swamp forests for oil palm plantation leads to increased loss of carbon via fluvial pathways, in addition to recognised increases in CO_2 emissions. Further, our data suggest that deeper drainage within plantations leads to greater DOC export, while the greater ^{14}C-inferred DOC age and higher $SUVA_{254}$ indicate that this C derives from deeper within the peat profile. Together with previous studies, our results suggest that the riverine export of DOC to coastal waters from peatland regions of Southeast Asia may have increased as a result of drainage and land conversion, with potentially profound (but as yet uncertain) impacts on coastal marine ecosystems via altered energy and nutrient supply, pH, and light regime (Durako et al., 2010; Frigstad et al., 2013; Traving et al., 2017).

With regard to the management of oil palm plantations on peatland, our measurements showed that all three Sabaju plantation sites had mean water table depths that were above the Roundtable on Sustainable Palm Oil's (RSPO) target range of 40 to 60 cm below the surface, whereas the Sebungan site fell within this range. While the Sabaju plantation had lower DOC fluxes and all sites had lower rates of DOC loss than the highly degraded peatland sites studies by Moore et al. (2013), the ^{14}C-depleted DOC measurements (relative to previous data from undrained peat swamp forests) obtained from all study sites indicate release of older stored carbon. This suggests that even RSPO-compliant plantations may still be expected to experience elevated fluvial loss of previously stored peat carbon, which is also indicative of drainage-induced C loss more generally (Evans et al., 2014). Managing oil palm plantations on peat to minimise both gaseous and fluvial carbon losses thus remains a significant challenge, requiring coordination among governments, the plantation industry, and academia (Wijedasa et al., 2016). However, our results suggesting relationships between drainage depth and DOC concentration and flux and ^{14}C-inferred source indicate that any measures that enable oil palm cultivation to be maintained at higher water levels should lead to commensurate reductions in peat carbon losses and would, therefore, lower the broader environmental impacts of oil palm cultivation.

Data availability. Data are available in Cook (2018).

Supplement. The supplement related to this article is available online at: https://doi.org/10.5194/bg-15-7435-2018-supplement.

References

Bjorkvald, L., Buffan, I., Laudon, H., and Morth, C.-M.: Hydrogeochemistry of Fe and Mn in small boreal streams: The role of seasonality, landscape type and scale, Geochim. Cosmochim. Ac., 72, 2789–2804, 2008

Campeau, A., Bishop, K., Billett, M. F., Garnett, M. H., Laudon, H., Leach, J. A., Nilsson, M. B., Öquist, M. G., and Wallin, M. B.: Aquatic export of young dissolved and gaseous carbon from a pristine boreal fen: implications for peat carbon stock stability, Global Change Biol., 23, 5523–5536, https://doi.org/10.1111/gcb.13815, 2017.

Carr, M. K. V.: The Water Relations and Irrigation Requirements of Oil Palm (Elaeis Guineensis): A Review, Exp. Agricult., 47, 629–652, https://doi.org/10.1017/s0014479711000494, 2011.

Catalan, N., Marce, R., Kothawala, D. N., and Tranvik, L. J.: Organic carbon decomposition rates controlled by water retention time across inland waters, Nat. Geosci., 9, 501–504, 2016.

Clark, J. M., Lane, S. N., Chapman, P. J., and Adamson, J. K.: Export of dissolved organic carbon from an upland peatland during storm events: Implications for flux estimates, J. Hydrol., 347, 438–447, 2007.

Cole, L. E. S., Bhagwat, S. A., and Willis, K. J.: Long-term disturbance dynamics and resilience of tropical peat swamp forests, J. Ecol., 103, 16–30, https://doi.org/10.1111/1365-2745.12329, 2015.

Cook, S., Peacock, M., Evans, C. D., Page, S. E., Whelan, M., Gauci, V., and Khoon, K. L.: Cold storage as

a method for the long-term preservation of tropical dissolved organic carbon (DOC), Mires and Peat., 18, 1–8, https://doi.org/10.19189/MaP.2016.OMB.249, 2016.

Cook, S.: Fluvial organic carbon losses from oil palm plantations on peat, https://doi.org/10.25392/leicester.data.7479575.v1, 2018.

Cory, R. M., Ward, C. P., Crump, B. C., and Kling, G. W.: Sunlight controls water column processing of carbon in arctic fresh waters, Science, 345, 925–928, https://doi.org/10.1126/science.1253119, 2014.

Couwenberg, J., Dommain, R., and Joosten, H.: Greenhouse gas fluxes from tropical peatlands in south-east Asia, Glob. Change Biol., 16, 1715–1732, https://doi.org/10.1111/j.1365-2486.2009.02016.x, 2010.

Dargie, G. C., Lewis, S. L., Lawson, I. T., Mitchard, E. T. A., Page, S. E., Bocko, Y. E., and Ifo, S. A.: Age, extent and carbon storage of the central Congo Basin peatland complex, Nature, 542, 86–90, 2017

Dommain, R., Couwenberg, J., and Joosten, H.: Development and carbon sequestration of tropical peat domes in south-east Asia: links to post-glacial sea-level changes and Holocene climate variability, Quat. Sci. Rev., 30, 999–1010, https://doi.org/10.1016/j.quascirev.2011.01.018, 2011.

Durako, M. J., Kowalczuk, P., Mallin, M. A., Cooper, W. J., Souza, J. J., and Wells, D. H.: Interannual Variation in Photosynthetically Significant Optical Properties and Water Quality in a Coastal Blackwater River Plume, Estuar. Coasts, 33, 1430–1441, https://doi.org/10.1007/s12237-010-9302-5, 2010.

Evans, C. D., Freeman, C., Cork, L. G., Thomas, D. N., Reynolds, B., Billett, M. F., Garnett, M. H., and Norris, D.: Evidence against recent climate-induced destabilisation of soil carbon from C^{14} analysis of riverine dissolved organic matter, Geophys. Res. Lett., 34, 1–5, https://doi.org/10.1029/2007GL029431, 2007.

Evans, C. D., Futter, M. N., Moldan, F., Valinia, S., Frogbrook, Z., and Kothawala, D. N.: Variability in organic carbon reactivity across lake residence time and trophic gradients, Nat. Geosci., 10, 832–835, https://doi.org/10.1038/ngeo3051, 2017.

Evans, C. D., Renou-Wilson, F., and Strack, M.: The role of waterborne carbon in the greenhouse gas balance of drained and re-wetted peatlands, Aquat Sci., 78, 573–590, 2016.

Evans, C. D., Page, S. E., Jones, T., Moore, S., Gauci, V., Laiho, R., Hruška, J., Allott, T. E. H., Billett, M. F., Tipping, E., Freeman, C., and Garnett, M. H.: Contrasting vulnerability of drained tropical and high-latitude peatlands to fluvial loss of stored carbon, Glob. Biogeochem. Cy., 28, 1215–1234, https://doi.org/10.1002/2013GB004782, 2014.

Farrar, D., Allen, B., Crump, K., and Shipp, A.: Evaluation of Uncertainty in Input Parameters to Pharmacokinetic Models and the Resulting Uncertainty in Output, Toxicol Lett., 49, 371–385, 1989.

Frigstad, H., Andersen, T., Hessen, D. O., Jeansson, E., Skogen, M., Naustvoll, L.-J., Miles, M. W., Johannessen, T., and Bellerby, R. G. J.: Long term trends in carbon, nutrients and stoichiometry in Norwegian costal waters: Evidence of regime shift, Prog. Oceanogr., 111, 113–124, 2013.

Gandaseca, S., Salimin, M. I., and Ahmed, O. H.: Effect of cultivation in different age's oil palm plantation on selected chemical properties of peat swamp soils, Agr. Forest. Fish., 3, 6–9, 2014.

Gandois, L., Cobb, A. R., Hei, I. C., Lim, L. B. L., Abu Salim, K., and Harvey, C. F.: Impact of deforestation on solid and dissolved organic matter characteristics of tropical peat forests: implications for carbon release, Biogeochemistry, 114, 183–199, https://doi.org/10.1007/s10533-012-9799-8, 2013.

Graneli, W., Lindell, M., and Tranvik, L.: Photo-oxidative production of dissolved inorganic carbon in lakes of different humic content, Limnol Oceanogr., 41, 698–706, 1996.

Gulliver, P., Waldron, S., Scott, E. M., and Bryant, C. L.: The Effect of Storage on the Radiocarbon, Stable Carbon and Nitrogen Isotopic Signatures and Concentrations of Riverine Dom., Radiocarbon, 52, 1113-01122, 2010.

Hirano, T., Segah, H., Kusin, K., Limin, S., Takahashi, H., and Osaki, M.: Effects of disturbances on the carbon balance of tropical peat swamp forests, Global Change Biol., 18, 3410–3422, https://doi.org/10.1111/j.1365-2486.2012.02793.x, 2012.

Hongve, D.: A Revised Procedure for Discharge Measurement by Means of the Salt Dilution Method, Hydrol. Proc., 1, 267–270, 1987.

Hooijer, A., Page, S., Canadell, J. G., Silvius, M., Kwadijk, J., Wösten, H., and Jauhiainen, J.: Current and future CO_2 emissions from drained peatlands in Southeast Asia, Biogeosciences, 7, 1505–1514, https://doi.org/10.5194/bg-7-1505-2010, 2010.

Hooijer, A., Page, S., Jauhiainen, J., Lee, W. A., Lu, X. X., Idris, A., and Anshari, G.: Subsidence and carbon loss in drained tropical peatlands, Biogeosciences, 9, 1053–1071, https://doi.org/10.5194/bg-9-1053-2012, 2012.

Hope, D., Billett, M. F., and Cresser, M. S.: A Review of the Export of Carbon in River Water – Fluxes and Processes, Environ. Pollut., 84, 301–324, 1994.

Hribljan, J. A., Kane, E. S., Pypker, T. G., and Chimner, R. A.: The effect of long-term water table manipulations on dissolved organic carbon dynamics in a poor fen peatland, J. Geophys. Res-Biogeo., 119, 577–595, https://doi.org/10.1002/2013JG002527, 2014.

Hudson, R. and Fraser, J.: Introduction to Salt Dilution Gauging for Streamflow Measurement Part IV: The Mass Balance (or Dry Injection) Method, Streamline Watershed Management Bulletin, 9, 6–12, 2002.

Husnain, H., Wigena, I. G. P., Dariah, A., Marwanto, S., Setyanto, P., and Agus, F.: CO_2 emissions from tropical drained peat in Sumatra, Indonesia, Mitig Adapt. Strat. Gl., 19, 845–862, 2014.

Iman, R. L. and Conover, W. J.: Small Sample Sensitivity Analysis Techniques for Computer Models, with an Application to Risk Assessment, Commun. Stat. Part A, Theory Meth., 1749–1842, 1980.

Jones, T. G., Evans, C. D., Jones, D. L., Hill, P. W., and Freeman, C.: Transformations in DOC along a source to sea continuum; impacts of photo-degradation, biological processes and mixing, Aquat. Sci., 78, 433–446, 2016.

Koehler, B., Landelius, T., Weyhenmeyer, G. A., Machida, N., and Tranvik, L. J.: Sunlight-induced carbon dioxide emissions from inland waters, Glob. Biogeochem. Cy., 28, 696–711, 2014.

Könönen, M., Jauhiainen, J., Laiho, R., Spetz, P., Kusin, K., Limin, S., and Vasander, H.: Land use increases the recalcitrance of tropical peat, Wetl. Ecol. Manage., 24, 717–731, 2016.

Logue, J. B., Stedmon, C. A., Kellerman, A. M., Nielsen, N. J., Andersson, A. F., Laudon, H., Lindstom, E. S., and Kriberg, E. S.: Experimental insights into the importance of aquatic bacterial

community composition to the degradation of dissolved organic matter, Isme J., 10, 533–545, 2016.

Matysek, M., Evers, S., Samuel, M. K., and Sjogersten, S.: High heterotrophic CO_2 emissions from a Malaysian oil palm plantations during dry-season, Wetl. Ecol. Manage., 26, 415–424, 2017.

Melling, L. and Henson, I. E.: Greenhouse Gas Exchange of Tropical Peatlands – a Review, J. Oil Palm., 23, 1087–1095, 2011.

Miettinen, J., Hooijer, A., Shi, C., Tollenaar, D., Vernimmen, R., Liew, S. C., Malins, C., and Page, S. E.: Extent of industrial plantations on Southeast Asian peatlands in 2010 with analysis of historical expansion and future projections, GCB Bioenergy., 4, 908–918, 2012a.

Miettinen, J., Hooijer, A., Tollenaar, D., Page, S., Malins, C., Vernimmen, R., Chi, C., and Liew, S. C.: Historical Analysis and Projection of Oil Palm Plantation Expansion on Peatland in Southeast Asia, Washington DC, International Council on Clean Transportation, 2012b.

Miettinen, J., Hooijer, A., Vernimmen, R., Liew, S. C., and Page, S. E.: From carbon sink to carbon source: extensive peat oxidation in insular Southeast Asia since 1990, Environ Res Lett., 12, 024014, 2017.

Miettinen, J., Shi, C. H., and Liew, S. C.: Deforestation rates in insular Southeast Asia between 2000 and 2010, Global Change Biol., 17, 2261–2270, https://doi.org/10.1111/j.1365-2486.2011.02398.x, 2011.

Miettinen, J., Shi, C. H., and Liew, S. C.: Land cover distribution in the peatlands of Peninsular Malaysia, Sumatra and Borneo in 2015 with changes since 1990, Glob. Ecol. Conserv., 6, 67–78, https://doi.org/10.1016/j.gecco.2016.02.004, 2016.

Monteith, J. L.: Evaporation and environment, P. Symp. Environ. Biol., 19, 205–234, 1965.

Moore, S., Evans, C. D., Page, S. E., Garnett, M. H., Jones, T. H., Freeman, C., Hooijer, A., Wiltshire, A., Limin, S., and Gauci, V.: Deep instability of deforested tropical peatlands revealed by fluvial organic carbon fluxes, Nature, 493, 660–664, 2013.

Moore, S., Gauci, V., Evans, C. D., and Page, S. E.: Fluvial organic carbon losses from a Bornean blackwater river, Biogeosciences, 8, 901–909, https://doi.org/10.5194/bg-8-901-2011, 2011.

Müller, D., Warneke, T., Rixen, T., Müller, M., Jamahari, S., Denis, N., Mujahid, A., and Notholt, J.: Lateral carbon fluxes and CO_2 outgassing from a tropical peat-draining river, Biogeosciences, 12, 5967–5979, https://doi.org/10.5194/bg-12-5967-2015, 2015.

Olefeldt, D., Roulet, N., Giesler, R., and Persson, A.: Total waterborne carbon export and DOC composition from ten nested subarctic peatland catchments – importance of peatland cover, groundwater influence, and inter-annual variability of precipitation patterns, Hydrol Proc., 27, 2280–2294, 2013.

Othman, H., Mohammed, A. T., Harun, M. H., Darus, F. M., and Mos, H.: Best management practises for oil palm planting on peat: optimum groundwater table, MPOB Information Series, 528, 1–7, 2010.

Page, S. E., Rieley, J. O., and Banks, C. J.: Global and regional importance of the tropical peatland carbon pool, Global Change Biol., 17, 798–818, 2011a.

Page, S. E., Morrison, R., Malins, C., Hooijer, A., Rieley, J. O., and Jauhiainen, J.: Review of peat surface greenhouse gas emissions from oil palm plantations in Southeast Asia (ICCT White Paper 15), International Council on Clean Transportation, Washington, 2011b.

Rixen, T., Baum, A., Wit, F., and Samiaji, J.: Carbon Leaching from Tropical Peat Soils and Consequences for Carbon Balances, Front Earth Sci., 4, https://doi.org/10.3389/feart.2016.00074, 2016.

Shafer, M. M., Perkins, D. A., Antkiewicz, D. S., Stone, E. A., Qurasishi, T. A., and Schauer, J. J.: Reactive oxygen species activity and chemical speciation of size-fractionated atmospheric particulate matter from Lahore, Pakistan: an important role for transition metals, J. Environ. Monitor., 12, 704–715, 2010.

Tiemeyer, B., Borraz, E. A., Augustin, J., Bechtold, M., Beetz, S., Beyer, C., Drosler, M., Elbi, M., Eickenscheidt, T., Fiedler, S., Forster, C., Freibauer, A., Giebels, M., Glatzel, S., Heinichen, J., Hoffman, M., Hoper, H., Jursinki, G., Leiber-Sauheitl, K., Peichl-Brak, M., Robkof, R., Sommer, M., and Zeitz, J.: High emissions of greenhouse gases from grasslands on peat and other organic soils., Global Change Biol., 22, 4134–4149, 2016.

Tipping, E., Corbishley, H. T., Koprivnjak, J. F., Lapworth, D. J., Miller, M. P., Vincent, C. D., and Hamilton-Taylor, J.: Quantification of natural DOM from UV absorption at two wavelengths, Environ. Chem., 6, 472–476, 2016.

Tonks, A. J., Aplin, P., Beriro, D. J., Cooper, H., Evers, S., Vane, C. H., and Sjogersten, S.: Impacts of conversion of tropical peat swamp forest to oil palm plantation on peat organic chemistry, physical properties and carbon stocks, Geoderma, 289, 36–45, 2017.

Traving, S. J., Rowe, O., Jakobsen, N. M., Sorensen, H., Dinasquet, J., Stedmon, C. A., Andersson, A., and Riemann, L.: The effect of increased loads of dissolved organic matter on estuarine microbial community composition and function, Front. Microbiol., 8, 351, https://doi.org/10.3389/fmicb.2017.00351, 2017.

Veloo, R., van Ranst, E., and Selliah, P.: Peat characteristics and its impact on oil palm yield, NJAS – Wagen J. Life Sc., 72–73, 33–40, 2015.

Weishaar, J. L., Aiken, G. R., Bergamaschi, B. A., Fram, M. S., Fujii, R., and Mopper, K.: Evaluation of specific ultraviolet absorbance as an indicator of the chemical composition and reactivity of dissolved organic carbon, Environ Sci. Tech., 37, 4702–4708, 2003.

Whelan, M. J. and Gandolfi, C.: Modelling of spatial controls on denitrification at the landscape scale, Hydrol. Proc. 16, 1437–1450, 2002.

Wicke, B., Dornburg, V., Junginger, M., and Faaij, A.: Different palm oil production systems for energy purposes and their greenhouse gas implications, Biomass Bioenerg., 32, 1322–1337, 2008.

Wijedasa, L. S., Page, S. E., Evans, C. D., and Osaki, M.: Time for responsible peatland agriculture, Science., 354, 562–562, 2016.

Wijedasa, L. S., Jauhiainen, J., Könönen, M., Lampela, M., Vasander, H., LeBlanc, M. C., Evers, S., Smith, T. E., Yule, C. M., and Varkkey, H.: Denial of long-term issues with agriculture on tropical peatlands will have devastating consequences, Global Change Biol., 23, 977–982, 2017.

Wijedasa, L. S., Sloan, S., Page, S. E., Clements, G. R., Lupascu, M., and Evans, T. A: Carbon emissions from Southeast Asia peatlands will increases despite emission-reduction schemes, Global Change Biol., 24, 4598–4613, https://doi.org/10.1111/gcb.14340, 2018.

Wit, F., Müller, D., Baum, A., Warneke, T., Pranowo, W. S., Müller, M., and Rixen, T.: The impact of disturbed peatlands on river outgassing in Southeast Asia, Nat. Com., 6, 10155, doi:10.1038/ncomms10155, 2015.

Yule, C. M.: Loss of biodiversity and ecosystem functioning in Indo-Malayan peat swamp forests, Biodivers. Conserv., 19, 393–409, 2010.

Yupi, H. M., Inoue, T., Bathgate, J., and Putra, R.: Concentrations, loads and yields of organic carbon from two tropical peat swamp forest streams in Riau Province, Sumatra, Indonesia, Mires and Peat, 18, doi:10.19189/MaP.2015.OMB.181, 2016.